Preferred conformations of the gas phase complex between Li+ and a model macrocycle tetraamide

2 AUTHORS:

Rubén D Parra
DePaul University
41 PUBLICATIONS 700 CITATIONS

SEE PROFILE

David L Cedeño
Millennium Pain Center
41 PUBLICATIONS 419 CITATIONS

SEE PROFILE

THEO
CHEM

Preferred conformations of the gas phase complex between Li$^+$ and a model macrocycle tetraamide

Rubén D. Parra [a,*], David L. Cedeño [b]

[a] Department of Chemistry, DePaul University, Chicago, IL 60614, United States
[b] Department of Chemistry, Illinois State University, Normal, IL 61790, United States

Abstract

The gas-phase binding of Li$^+$ by a model macrocycle tetraamide, via its amide C=O groups, is investigated using ab initio methods. The macrocycle ligand contains four amide units linked by alternating phenyl and ethenyl groups. Geometries and vibrational frequencies for the complexes are obtained at the B3LYP/6-31G(d) level. Geometries are further optimized at the B3LYP/6-31+G(d) level. Interaction energies, corrected for basis set superposition error, are evaluated using the MP2 method with the 6-31+G(d) and 6-311+G(d) basis sets. It is found that the model tetraamide presents enough flexibility to bind the Li$^+$ metal ion in at least four different conformations characterized by their group symmetries C_s, C_2, C_{2h}, and C_{2v}. The respective interaction energies are close to one another with an average value of −79.40 kcal/mol at the MP2/6-311+G(d) level. Natural bond orbital analysis (NBO) is performed to investigate the extent of ligand polarization and charge-transfer (CT) interactions in the various conformations of the complex. Extended conformational searches for the free macrocycle tetraamide, and its Li$^+$ complex conformations are conducted using a Monte Carlo-based analysis with the PM3 semiempirical method and compared with the B3LYP results via similarity calculations.
© 2007 Elsevier B.V. All rights reserved.

Keywords: Ab initio; Gas-phase binding of metal ions; NBO analysis; Conformational search; Macrocycle tetraamides

1. Introduction

The development of ion receptors, also known as ionophores, is of great significance because of the fundamental role of ions in many chemical and biological processes [1]. A better understanding of ion-receptor interactions results in more efficient designs of ionophores with specific applications. For example, the increasing need of properly disposing of nuclear waste has led to the creative design of ionophores capable of binding radioactive ions to separate them from others [2]. Also, several other ion receptors have been designed for medicine [3], and pollution monitoring [4].

Macrocyclic ionophores are particular hosts capable of forming stable complexes with charged species by providing many binding sites directed toward the guest in a convergent manner. Perhaps the most widely known and extensively investigated macrocyclic ionophores are the so-called crown ethers and analogous which exhibit strong affinity and high selectivity for alkali and alkaline metal ions [5]. Some other widely investigated macrocyclic hosts include cryptands [6], starands [7,8], cyclodextrines [9], and calixarenes [10]. Macrocyclic polyamides form another group of ion receptors that have been given considerable attention [11]. The notable solubility in organic solvents usually accompanied by a diminished solubility in aqueous solution makes amides appealing for applications in the field of ion-selective electrodes and liquid–liquid separations. Additionally, the hydrogen bonding capabilities of amides are known to be crucial in many relevant systems including enzymes and proteins. Much effort has been devoted in the design of novel charged and neutral macrocycle tetraamides for anion recognition [11a,11b,11c,11d,11e,11f]. The complexation of

* Corresponding author. Tel.: +1 773 325 4343; fax: +1 773 325 7421.
E-mail address: rparra1@depaul.edu (R.D. Parra).

alkali and transition metal ions by macrocyclic tetraamides has also been the subject of recent publications by several authors [11g,11h,11i,11j]. The important role played by proteins in the transportation of ions has prompted some researchers to study the binding properties of cyclic peptides [12]. Such studies demonstrated that the cyclic peptides are flexible enough to allow for either cation or anion binding despite the rigidity of the amide group. Thus, the amide group exhibits desirable amphiphilic properties with the carbonyl group serving as a suitable binding site for metal ions, and the N—H group serving as a binding site for anions [13,14].

In a recent ab initio study, the equilibrium geometries and relative stabilities of four clearly distinct conformations of a model macrocycle tetraamide were reported [15]. The four amide groups are found in the general sequence —L1—[NHCO]—L2—[CONH]—L1—[NHCO]—L2—[CONH]—, where the phenyl group was chosen for L1 and the ethenyl group for L2. Here, L1 links two amide groups trough covalent bonding of the nitrogen atoms specifically in the positions 1 and 3 of the phenyl group. Similarly, L2 links two amide groups by covalent bonding to the carbonyl carbon atoms. It is noteworthy that macrocycle tetraamides with the above general sequence, with different linkers L1 and L2, have been experimentally studied by other researchers [11]. The most relevant study is that of Singh et al. [11l], who reported the synthesis and biochemical activity of manganese and iron complexes with macrocycle tetraamides; for one of these macrocycles the L1 used, a phenyl group, was the same as the L1 used in our model system, and the L2 was a phenyl group binding the carbonyl carbons in the 1 and 2 positions, which is therefore very close to our L2. Other experimental and closely related studies are those by Jurczak et al. [11a], where L1 = $(CH_2)_n$ ($n = 2$–5), and L2 = pyridine (binding the C=O groups in the 1 and 3 position of pyridine); Still et al. [11k], where L1 = cyclohexane (binding the NH groups in positions 1 and 2), and L2 = phenyl (binding the C=O groups in positions 1 and 3). The present study expands on the previous work by investigating, via ab initio calculations, the structural transformations and accompanying electron density redistribution of the model macrocyclic tetraamide upon gas-phase binding of an alkali metal ion, more specifically the Li^+ ion. It should be noted that in the tetraamide complexes with iron and manganese reported by Sing et al. [11l], the metal ions are proposed to have octahedral coordination with four coordination sites provided by the tetraamide via its amide nitrogens, and two Cl^- bonded to the metal ions. In this study, we evaluate the ability of the tetraamide model to bind metal ions via its carbonyl oxygen atoms, and thus expand its potential usefulness. Natural bond orbital analysis (NBO) is performed to investigate the energetic importance of ligand polarization and charge-transfer (CT) interactions. Conformational searches are also performed for both the free macrocycle and its Li^+ complexes using a Monte Carlo-based analysis and the PM3 semiempirical method.

2. Methods of calculations

Ab initio calculations were carried out with the GAUSSIAN 03 program [16]. Geometry optimizations and frequency calculations were first performed at the B3LYP [17] level using the 6-31G(d) [18]. The geometries were further optimized using the 6-31+G(d) basis set [19]. Single-point energy calculations were performed using the 6-31+G(d), and 6-311+G(d) [20] basis sets at the MP2 level [21]. The optimized geometries were subjected to natural bond orbital (NBO) analysis performed on wave functions calculated at the HF/6-31+G(d,p) level [22]. The interaction energies reported here were corrected for basis set superposition error (BSSE) using the counterpoise method of Boys and Bernardi [23]. Conformational searches were carried out using a Monte Carlo-based analysis with the PM3 semiempirical method as implemented in Spartan'04 and Spartan'06 for Windows [24]. Initial geometries were taken from Parra et al. [15], which were the results of geometry optimizations using density functional theory (B3LYP) with the 6-31+G(d) basis set. These geometries were also used as initial guess geometries for geometry optimization under the PM3 semiempirical method. Similarity calculations were carried out to quantify the extent of similarity of the results obtained from the expanded conformational searches and the DFT results.

3. Results and discussion

3.1. Uncomplexed macrocycle tetraamide

In a previous study [15], a limited B3LYP/6-31+G(d) search for stable conformations of the model macrocycle tetraamide resulted in the identification of four clearly distinct minimum-energy structures that were labeled AA_1, AA_2, BC_1, and BC_2. In this work, these labels are respectively replaced by the more compact labeling M1, M2, M3, and M4. The relative electronic energies at the MP2/6-31+G(d,p) level were reported to be M1 (0.00 kcal/mol) < M2 (0.86 kcal/mol) < M3 (2.09 kcal/mol) << M4 (9.17 kcal/mol). We decided to expand the conformational search of the free macrocycle using a Monte Carlo-based analysis with the PM3 semiempirical method as implemented in Spartan'04 and '06 for Windows [24]. The DFT minimum-energy structures were used as initial guess geometries for both PM3 geometry optimizations and conformationals searches. The main purpose of the optimization under PM3 conditions is to carry out a broader search for minima. Geometry optimizations using the PM3 semiempirical method resulted in conformations fairly close to those obtained using DFT for the M1 (C_i), M2 (C_2), and M3 (C_s) ligands. The similarities are above 90% with small differences found mostly on the tilt angle of the benzene rings relative to the ethylene moieties. In contrast, the M4 (C_s) geometry was notoriously different, only 76% similar to the DFT geometry. The difference is

due to the tilting of a benzene ring in the direction opposite to that found in the DFT optimization.

3.2. Conformational searches of the free macrocycle

3.2.1. M1 conformer

The PM3 Monte Carlo search found five low energy conformations using the DFT optimized M1 conformation as initial guess geometry. The four lowest energy conformations are all close to one another (within 2 kcal/mol), and the highest energy conformation is 5.7 kcal/mol above the lowest energy conformation. The three lowest energy conformations are reasonably similar to one another (above 90%), but not very similar to the DFT geometry (between 75% and 85%). The lowest energy conformer is only 76% similar to the DFT geometry. The conformer that is most similar (96%) to the DFT geometry is the fourth in increasing energy, which is only 1.5 kcal/mol above the lowest energy conformation. Chart 1 shows the lowest energy conformer, and the one that is most similar to the DFT geometries. Note that the lowest energy conformer adopts a geometry that resembles more that of the M2 conformer.

3.2.2. M2 conformer

A total of fourteen low energy conformers were found in this case. The seven lowest energy conformers are all within 2 kcal/mol. The eighth conformer is 3.5 kcal/mol above the lowest, and the remaining six conformers are above the lowest energy conformer by more than 5.3 kcal/mol.

The lowest energy conformer is 91% similar to the DFT geometry, but the most similar is the second lowest conformer (98%). Chart 1 shows their geometries. Both conformers are similar, except for the amount of tilting of the benzene rings relative to each other. The lowest energy conformer seems to be more concave than the one that is most similar to the DFT geometry.

3.2.3. M3 conformer

This search yielded fourteen low energy conformers. The twelve lowest energy conformers differ by less than 2 kcal/mol. The seventh conformer, 96% similar to the one obtained with DFT, is only 0.4 kcal/mol above the lowest energy conformer. Moreover, the lowest energy conformer is also very similar (91%) to the DFT optimized geometry (See Chart 1).

3.2.4. M4 conformer

In this case, the search yielded nine low energy conformers. The seven lowest energy conformers differ by less than 2 kcal/mol, while the two highest ones are almost 3 kcal/mol above the lowest energy one. Most of the conformers are not very similar to the DFT geometry. For example, the lowest energy one is quite distorted being only 75% similar to the DFT geometry. The most similar is the third lowest energy conformer as shown in Chart 1.

In short, conformational searches starting with the M1 and M2 DFT geometries yielded a lowest energy conformer that resembles the DFT optimized geometry of the M2 conformation. The PM3 Monte Carlo relative

M1: DFT geometry   PM3 lowest energy (76%)   PM3 most similar (96%)

M2: DFT geometry   PM3 lowest energy (91%)   PM3 most similar (98%)

M3: DFT geometry   PM3 lowest energy (91%)   PM3 most similar (96%)

M4: DFT geometry   PM3 lowest energy (75%)   PM3-most similar (91%)

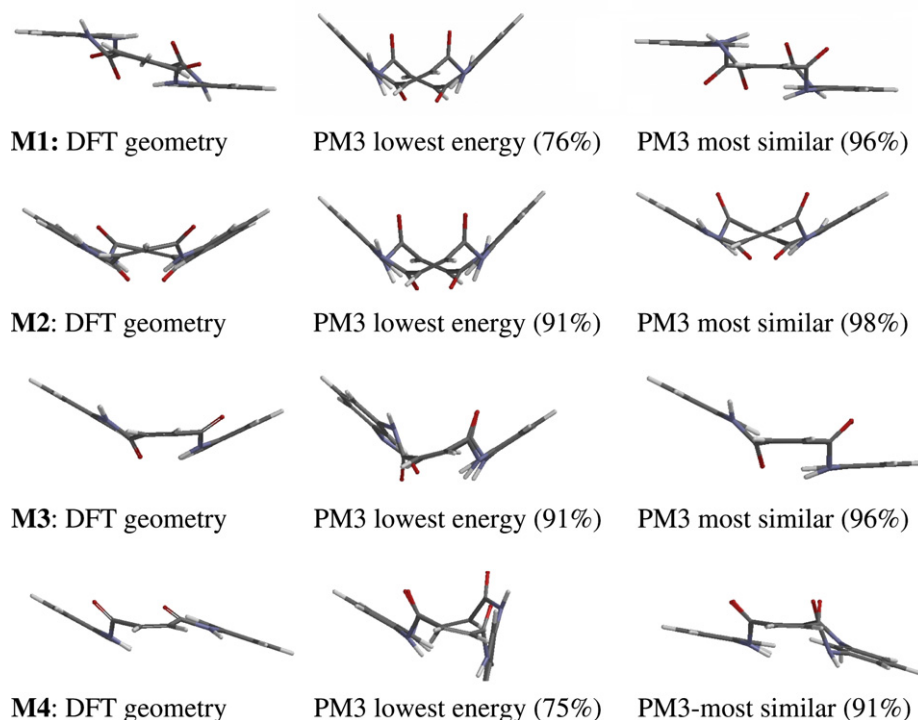Chart 1.

energies of the conformations closest to the DFT results are in the order M2 (0.0 kcal/mol) < M1 ∼ M3 (1.0–1.5 kcal/mol) < M4 (∼4.0 kcal/mol).

3.2.5. Li^+-complexes

The stability of the free macrocycle has been traced down to the presence of both N—H...O=C and C—H...O=C intramolecular hydrogen bonds [15]. Accordingly, binding a metal-ion guest via the C=O groups will involve the breaking of at least the N—H...O=C interactions along with proper geometry readjustment of the C=O groups. Four minimum-energy structures were found for the interaction of the Li^+ cation and the macrocycle tetraamide via its amide C=O groups. Selected geometry parameters are based on the labeling scheme shown Fig. 1. Based on their corresponding point groups, the structures are conveniently labeled Li-C_{2h}, Li-C_{2v}, Li-C_2, and Li-C_s. Fig. 2 shows a side view of each structure, and Fig. 3 shows the corresponding top view. Relevant geometrical parameters are given in Table 1, and interaction energies are given in Table 2. Except for Li-C_2, the four amide oxygen atoms lie in a plane, and the four carbon atoms of the two ethenyl groups lie in another plane. The deviation from planarity in Li-C_2 is indicated by dihedral angles of −48° and 39° for the amide oxygens and the ethenyl carbons, respectively. The Li^+ ion sits perfectly on the center of the rectangular plane defined by the oxygen atoms in Li-C_{2h}, as implied by the symmetric Li^+...O distances of 2.052 Å, and the O_1...Li^+...O_3 angles of 180°. Li-C_{2v} also shows the Li^+ ion with identical Li^+...O distances of 2.033 Å; however, the metal ion is located now above the plane of the oxygen atoms with O_1...Li^+...O_3 angles of 157°. The local geometry defined by the oxygen atoms and the metal ion is then pyramidal with a rectangu-
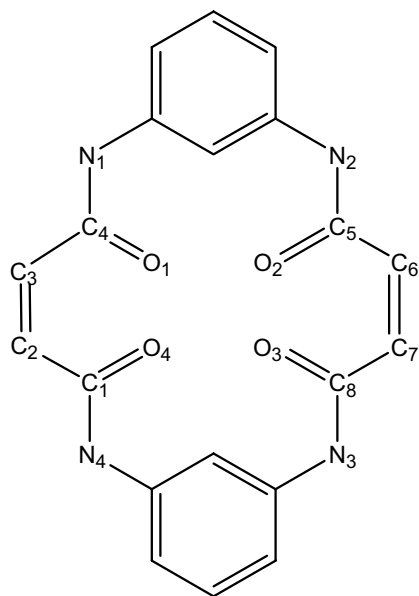

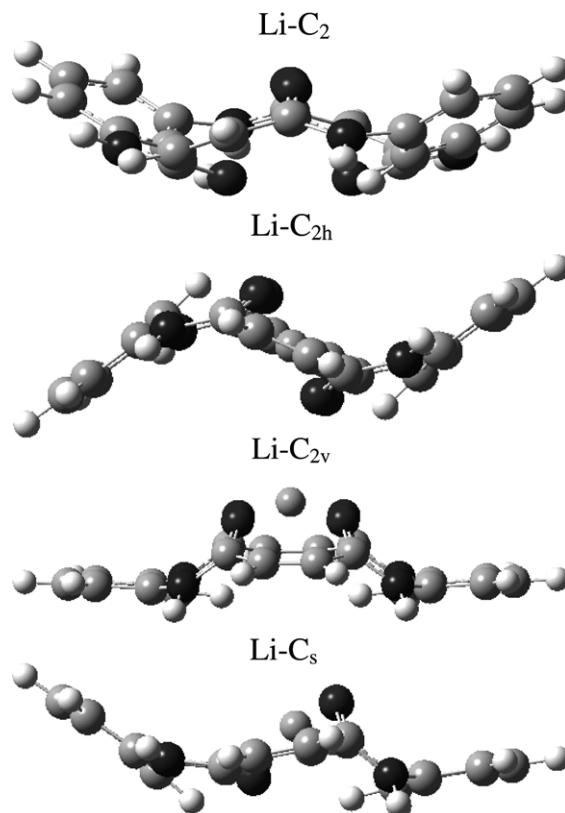
Fig. 2. Side view of the various Li–macrocycle complexes.

lar base. One striking difference between Li-C_{2h} and Li-C_{2v} is seen in the relative orientations of the phenyl rings. In the former the phenyl rings are parallel to each other, while in the latter they are essentially coplanar. In Li-C_s, the metal ion binds asymmetrically to the four oxygen atoms with Li^+...O distances of 2.024 Å and 2.125 Å. Also, the Li^+ ion lies above the plane of the oxygen atoms with O_1...Li^+...O_3 angles of 160°. In Li-C_2, the metal ion binds asymmetrically to the four oxygen atoms with Li^+...O distances of 1.972 Å and 2.029 Å. The local geometry of the four oxygen atoms and the metal ion in Li-C_2 resembles a distorted tetrahedron.

Interaction energies calculated at the MP2/6-31+G(d) and MP2/6-311+G(d) level on the B3LYP/6-31+G(d) optimized geometries are presented in Table 2. The interaction enthalpies determined using the B3LYP/6-31G(d) harmonic frequencies are also shown in Table 2. Despite the lack of pre-organization of the free macrocycle, the average magnitude of the interaction enthalpies is large, 77.66 kcal/mol at the MP2/6-311+G(d) level. The interaction enthalpies in the various conformations follow the order Li-C_2 > Li-C_s > Li-C_{2v} > Li-C_{2h}.

4. NBO analysis

Natural bond orbital analysis (NBO) was performed for the various conformations of the metal ion complex to investigate the extent of ligand polarization and charge-transfer (CT) interactions. The calculations were carried
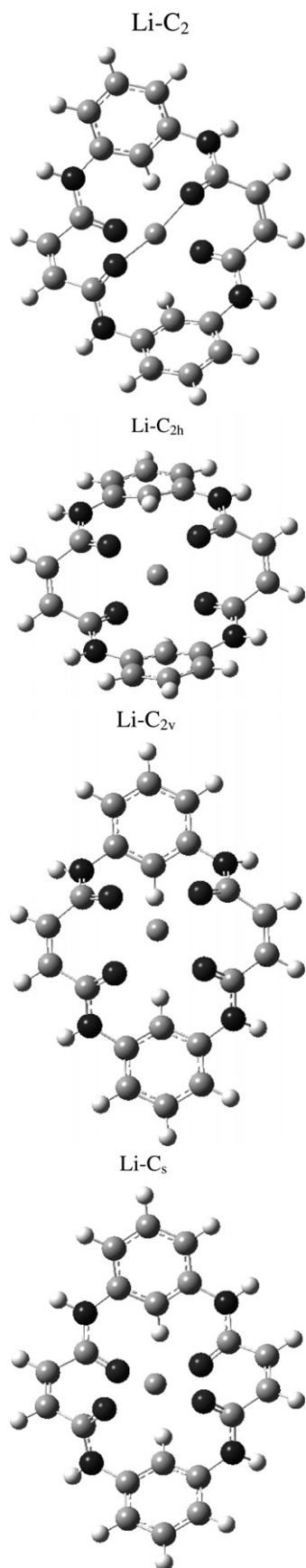

Fig. 1. Labeling scheme shown for discussion of selected geometry parameters.

Li-C₂

Li-C₂ₕ

Li-C₂ᵥ

Li-Cₛ

Fig. 3. Top view of the various Li–macrocycle complexes structures.

Table 1
Selected bond lengths (Å) and angles (°) for the Li⁺–macrocycle complexes

	Li-C_{2v}	Li -C_2	Li-C_{2h}	Li -C_s
$O_1 \ldots O_2$	2.988	3.610	3.132	3.388
$O_1 \ldots O_3$	3.981	3.615	4.105	4.086
$O_1 \ldots O_4$	2.630	2.675	2.654	2.655
$O_2 \ldots O_3$	2.630	2.675	2.654	2.655
$O_2 \ldots O_4$	3.981	3.075	4.105	4.086
$O_3 \ldots O_4$	2.988	3.610	3.132	2.847
$O_1 \ldots M$	2.033	1.972	2.052	2.024
$O_2 \ldots M$	2.033	2.029	2.052	2.024
$O_3 \ldots M$	2.033	1.972	2.052	2.125
$O_4 \ldots M$	2.033	2.029	2.052	2.125
$O_1 \ldots M \ldots O_2$	94.6	128.9	99.4	113.7
$O_1 \ldots M \ldots O_3$	156.6	132.9	180.0	160.1
$O_1 \ldots M \ldots O_4$	80.6	83.9	80.6	79.5
$O_2 \ldots M \ldots O_3$	80.6	83.9	80.6	79.5
$O_2 \ldots M \ldots O_4$	156.6	98.5	180.0	160.1
$O_3 \ldots M \ldots O_4$	94.6	128.9	99.4	84.1
$O_1 O_2 O_3 O_4$	0	−48	0	0
$O_1 C_4 C_3 C_2$	37.8	41.4	−39.3	59.8
$O_4 C_1 C_2 C_3$	−37.8	32.5	−39.3	17.4
$C_2 C_3 C_6 C_7$	0.0	39.2	0.0	0.0

Table 2
MP2 interaction energies and enthalpies (kcal/mol) of the Li⁺–macrocycle complexes

	6-31+G(d)		6-311+G(d)	
	ΔE^{a}	ΔH^{b}	ΔE^{a}	ΔH^{b}
Li-C_{2v}	−78.28	−76.87	−78.69	−77.28
Li-C_2	−84.00	−82.15	−82.91	−81.06
Li-C_s	−80.95	−79.30	−79.85	−78.20
Li-C_{2h}	−78.35	−76.27	−76.16	−74.08

[a] Counterpoise-corrected interaction energies relative to the fully optimized uncomplexed macrocycle M1, of symmetry C_i.
[b] Enthalpy corrections (298 K) are determined using the B3LYP/6-31G(d) harmonic frequencies, and include the counterpoise correction for all entries.

out at the HF/6-31+G(d,p) level using the B3LYP/6-31+G(d) optimized geometries. Table 3 lists the NBO atomic charges of the metal ion in a given complex conformation, the average atomic charges of the oxygen atoms in the complex, and the average group charge for the CNH atoms of the amide motif. Also shown in Table 3 are the corresponding charge values in the macrocycle tetraamide (geometry same as in the complex) but in the absence of the metal ion. Charge values for the free fully optimized macrocycle are given in the caption of Table 3. Table 4 shows the results from the second-order perturbation theory analysis of the Fock matrix within the NBO basis.

As seen in Table 3, the overall effect of forming a metal-ion complex is the gain of electron density by the metal with a concomitant loss of electron density by the macrocycle tetraamide. In each case, the charge in the metal ion polarizes electrons in the macrocycle toward the oxygen centers resulting in a more favorable electrostatic interaction with the metal ion. In particular, the average percent increase of electron density in the amide oxygen atoms is matched very closely by the average percent loss of electron

Table 3
HF/6-31+G(d,p) dipole moments (Debyes), NBO atomic and group charges (au)

	Li[+a]	$\langle q_O \rangle^a$	$\langle q_{CNH} \rangle^a$	$\langle q_O \rangle^b$	$\langle q_{CNH} \rangle^b$	$\%\Delta\langle q_O \rangle$ (%)[c]	$\%\Delta\langle q_{CNH} \rangle$ (%)[c]	μ^a	μ^b
Li-C$_2$	0.907	−0.797	0.592	−0.677	0.496	18	19	0.07	0.92
Li-C$_s$	0.919	−0.797	0.588	−0.681	0.498	17	18	1.39	3.31
Li-C$_{2v}$	0.931	−0.772	0.556	−0.627	0.455	23	22	5.19	8.46
Li-C$_{2h}$	0.915	−0.790	0.601	−0.673	0.510	17	18	0.00	0.00

[a] Properties calculated on the B3LYP/6-31+G(d) optimized complexes.
[b] Free ligand with geometry as in the complex. The corresponding values for the optimized macrocycle are $\langle q_o \rangle = -0.731$, $\langle q_{CNH} \rangle = 0.535$, and $\mu = 0.00$ D.
[c] % Change going from free macrocycle (geometry same as in complex) to metal-ion complex.

Table 4
Results from the second-order perturbation theory analysis within the NBO basis for the Li^{+} complexes at the HF/6-31+G(d,p) level of theory[a]

	$[\sum\Delta E_{no\to Li^+}]/4$ [b]	$\langle q_{o\to Li^+} \rangle^c$	q_{Li^+} (estimated)[d]	q_{Li^+} (actual)	$\sum\Delta E_{no\to Li^+}/\sum\Delta E_{ij}$ (%)
Li-C$_2$	15.55	0.022	0.911	0.907	59
Li-C$_s$	12.34	0.019	0.926	0.919	56
Li-C$_{2v}$	13.22	0.017	0.933	0.931	69
Li-C$_{2h}$	9.65	0.014	0.943	0.915	38

[a] Properties calculated on the B3LYP/6-31+G(d) optimized complexes.
[b] Sum of delocalization energies (kcal/mol) of the oxygens lone pairs into "empty" non-Lewis NBOs in the metal ion averaged over the total number of oxygen atoms.
[c] Quantity of charge (e) transferred from the lone pairs of the oxygen atoms to the acceptor orbitals in the metal ions averaged over the total number of oxygen atoms.
[d] Metal ion charge estimated using the transferred charge from the oxygen atoms: $q_{Li^+} \approx 1.00 - 4\langle q_{o\to Li^+} \rangle$.

density in the amide CNH group. The NBO charges also reveal the unfavorable O...O interactions occurring in the different conformations of the macrocycle complexes. By adopting a more convenient binding geometry, the oxygen atoms get closer to one another which results in repulsive O...O interactions. To minimize such repulsion, a sizeable amount of electron density is drawn away from the oxygen atoms toward the CNH group. The effect is more evident when the macrocycle adopts the C$_{2v}$ structure with about 14% reduction in the magnitude of the average oxygen atomic charge, $\langle q_O \rangle$, with a similar reduction in the magnitude of the average $\langle q_{CNH} \rangle$ group charge.

The redistribution of electron density in the macrocycle is expected to induce a net permanent dipole moment in the molecule, unless the effect is cancelled by symmetry. This expectation is confirmed by the calculated dipole moments displayed in Table 3. Except for Li-C$_2$ and Li-C$_{2h}$, the other two conformations possess relatively large dipole moments. Moreover, the dipole moments of the uncomplexed ligand with the same geometry as in the complex are reduced upon binding of the metal ion. This ion-induced reduction of the dipole moment demonstrates the important role played by the ion-dipole interactions in the overall stability of the complexes. In account of its large dipole moment, the Li-C$_{2v}$ complex is expected to be dominant in polar solvents.

The energetic importance of the interaction between "filled" (electron-donor) Lewis-type NBOs and "empty" (electron-acceptor) non-Lewis NBOs may be estimated by second-order perturbation theory. Of particular importance is the stabilization of the complex gained by delocal-

ization of the oxygen lone pairs into suitable orbitals in the corresponding metal-ion guest, no→Li^{+}. The delocalization energies $E^{(2)}$ can be approximated by the expression [22],

$$E^{(2)} = \Delta E_{ij} \approx -2.\frac{F(i,j)^2}{\varepsilon_j - \varepsilon_i}$$

where ε_i and ε_j are acceptor and donor orbital energies, and $F(i,j)$ is the off-diagonal NBO Fock matrix element. Table 4 shows the sum of the $\Delta E_{no—Li^+}$ values averaged over the total number of oxygen atoms. It is seen that Li-C$_2$ is the conformation with the greatest stabilization, while Li-C$_{2h}$ is the one with the smallest stabilization in accordance with the complex interaction energies shown in Table 2. Similarly, Li-C$_{2v}$ and Li-C$_s$ average delocalization energies are within 1.00 kcal/mol, a result that mirrors the corresponding interaction enthalpies. The quantities of transferred charge from the lone pairs of the oxygen atom to the acceptor orbitals in the metal ion can be estimated using the approximate formula

$$q_{d\to a} \approx 2.\left(\frac{F(i,j)}{\varepsilon_j - \varepsilon_i}\right)^2$$

The results, averaged over the number of oxygen atoms, reported in Table 4 indicate sizeable charge transfer with the largest transfer occurring for Li-C$_2$ and the smallest for Li-C$_{2h}$. The charge of the metal ion in a complex can then be estimated based on the amount of electron charge transferred from the oxygen atoms to the ion as follows

$$(q_{Li^+})_{estimated} = +1.000 - 4\langle q_{O\to Li^+} \rangle$$

The difference between the estimated and the actual charge of the metal ion specifies the quantity of charge being transferred from the macrocycle through atoms other than the amide oxygen atoms. Particularly striking are the results in the Li-C_{2h} complex where the difference between the estimated and actual charge of the Li$^+$ ion is twice as much the average charge transferred from the oxygen atoms; this results is in sharp contrast with those of the other complex conformations.

The relative importance of the contribution made by the lone pairs of the oxygen atoms, $\sum \Delta E_{no \rightarrow M^+}$, to the overall stabilization energy $\sum \Delta E_{ij}$ can be gleaned from Table 4, which shows the percent ratio of the two quantities. The percent contribution of the oxygen lone pairs grows as the metal ion gets farther away from both the phenyl and the ethene bridge units. For example, while delocalization of the oxygen lone pairs contributes greatly (69%) to the overall stabilization energy in Li-C_{2v}, such contribution is substantially smaller (38%) in Li-C_{2h}. The results are consistent with the relative amounts of charge transferred and the geometries of the conformations since, as shown in Fig. 3, the metal ion in Li-C_{2h} is located at the center of symmetry of the complex and it is in closer contact with more atoms of the macrocycle tetraamide than in Li-C_{2v}. In fact, the metal ion in Li-C_{2v} is above the plane of the ethene carbons, and thus relatively far from the phenyl rings, which helps to explain why the major source of the overall stabilization energy is the delocalization of the oxygen lone pairs.

5. Binding affinity

The energy results displayed in Table 2 show that the model macrocycle tetraamide has metal-ion binding affinities comparable to other well-studied hosts such as the 12-C4 and 18-C6 crown ethers. In the case of the 12-C4 crown ether, ab initio gas-phase interaction energies with Li$^+$ of -82.4 kcal/mol (D_{2d}), and -86.8 kcal/mol (C_4) were reported by Cui et al. [7]. The values reported by Cui et al. are akin to those in Table 2. Cui et al. found ion-dipole interactions to be crucial in the 12-C4 metal ion complexes of C_4 symmetry having a volcano shape and with the metal ion located above the volcano akin to the Li-C_{2v} complex of the model macrocycle tetraamide. As found in the 12-C4 complexes, ion-dipole interactions are important for the external binding in the Li-C_{2v}. In the case of the 18-C6 crown ether, ab initio gas-phase interaction energies with Li$^+$ were reported by Glendening et al. [5c]. The HF/6-31+G(d) (BSSE-corrected) results for the Li$^+$ complexes are: -89.1 kcal/mol (S_6) and -86.8 kcal/mol (D_{3d}). Compared with both 12-C4 and the model macrocycle tetraamide, 18-C6 presents a somewhat superior attraction toward Li$^+$ partly due to the additional pair of oxygen atoms. Very relevant results are those reported by Kim et al. for the binding of Li$^+$ by novel amphi-ionophores of cyclic tetrapeptides and hexapeptides composed of glycine molecules [12c]. The interaction energies, calculated at the B3LYP/6-31+G(d) level using geometries optimized with the same basis set and the HF method, are -63.6 and -98.1 kcal/mol for the tetrapetide and hexapeptide, respectively. Interestingly, the average interaction energy of the model macrocycle tetraamide complex with Li$^+$ (-77.66 kcal/mol) is close to the mean value of the tetra and hexapeptide results reported by Kim (-80.85 kcal/mol). Recently, Suh et al. [12a] reported the binding affinities for Li$^+$ by a novel amphi-ionophore cyclohexapeptide composed of six alanine molecules. The HF/6-31+G(d) BSSE-corrected interactions energies are -100.0 kcal/mol; these authors also reported MP2/6-31+G(d) results of -102.1 kcal/mol. The results evince the cation binding affinities of the amide motif, which tend to increase with the number of amide groups in the host.
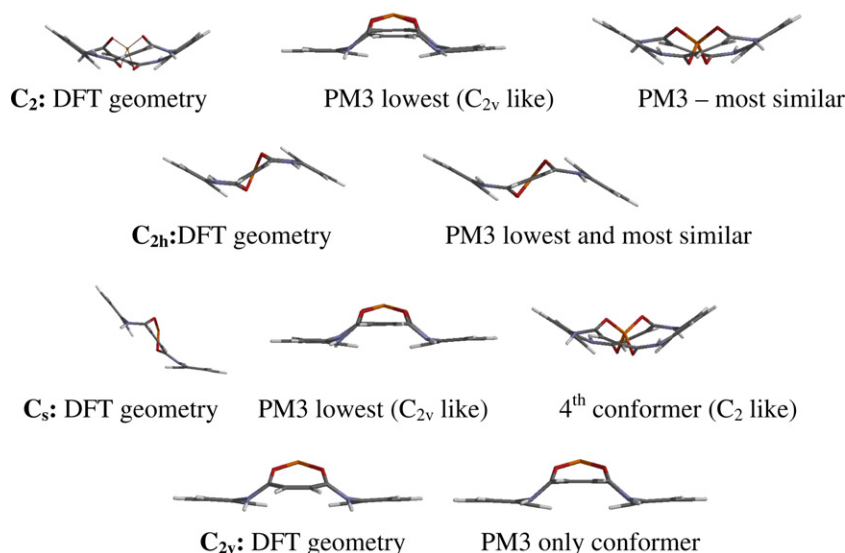

C$_2$: DFT geometry   PM3 lowest (C$_{2v}$ like)   PM3 – most similar

C$_{2h}$: DFT geometry   PM3 lowest and most similar

C$_s$: DFT geometry   PM3 lowest (C$_{2v}$ like)   4th conformer (C$_2$ like)

C$_{2v}$: DFT geometry   PM3 only conformer

Chart 2.

6. Conformational searches on complexes

PM3 Monte Carlo conformational searches were carried out starting with the four different conformations discussed above. Chart 2 shows the DFT geometries with the ones resulting from the conformational PM3 search (lowest energy and most similar). These are noted by the symmetry group symbol to what the DFT geometry belongs. The C_2, C_{2h}, and C_{2v} conformation are not significantly altered upon PM3 optimization. However, PM3 optimization of the C_s symmetry complex resulted in the C_{2v} conformer.

6.1. Li-C_2 complex

The conformational search that started with the DFT geometry of this complex yielded four low energy conformers all within 1 kcal/mol. Three of the conformers are virtually identical to one another (similarity score is 100%) and close to the fourth conformer (82% similar). As shown in Chart 2, the lowest energy conformer is similar to the C_{2v} conformer. The conformer most similar to the DFT geometry is the third lowest, which is only 0.25 kcal/mol above the lowest C_{2v} conformer.

6.2. Li-C_{2h} complex

The conformational search found seven low energy conformers. Five of them do not differ by more than 1 kcal/mol relative to the lowest energy. The other two are about 2.3 kcal/mol above the lowest energy one. The lowest energy one is also the most similar to the DFT geometry (100%). This conformer is about 9.5 kcal/mol above the C_{2v} conformer that was found as the lowest energy conformer in the other searches. Chart 2 illustrates its geometry.

6.3. Li-C_s complex

Six low energy complexes were found in this search. None of the conformers are similar to the DFT optimized geometry; a result consistent with a PM3 optimization that diverged from the C_s symmetry to give the C_{2v} conformer. The four lowest conformations are within only 0.2 kcal/mol from one another. The fifth and sixth conformers are 1.0 and 5.6 kcal/mol above the lowest energy one. The PM3 conformational search finds the lowest energy conformer to be specially similar to the C_{2v} conformer. Interestingly, the fourth conformer, in increasing energy, is similar to the C_2 (although it seems to be a stereoisomer), while the highest energy conformer resembles the C_{2h}, even though one of the benzene rings is tilted in the opposite direction.

6.4. Li-C_{2v} complex

The conformational search found solely one conformer similar to the DFT optimized conformer in agreement with two of the other three searches that also located a C_{2v} conformer as the lowest energy one.

The Monte Carlo-based analysis with the PM3 semiempirical method enables us to say that the Li$^+$ complex prefers a C_{2v} symmetry arrangement in which the ion sits on top of four carbonyls. The C_2 conformation is also possible although it has slightly larger energy (0.3–1.0 kcal/mol). The C_{2h} conformation is also likely, but it is about 10 kcal/mol above the other two. Finally, the C_s conformation appears so close to the C_{2v} conformation that it could not be located in the PM3 surface. Inspection of Table 2 confirms that the Li-C_{2v} and Li-C_s conformations have indeed interaction enthalpies that are comparable within 1.08 kcal/mol at the MP2/6-311+G(d) level.

7. Summary and outlook

An ab initio study has been presented for the interaction geometries and corresponding binding energies of a model macrocycle tetraamide with the metal ion Li$^+$. Four minimum-energy structures were found for the interaction of Li$^+$ and the macrocycle tetraamide via its amide C=O groups. Though lacking pre-organization, the model macrocycle exhibits affinity for the metal ion comparable to that of 12-C4 crown ether and cyclic tetrapeptides [7,12c]. As found in the 12-C4 complexes with Li$^+$, ion-dipole interactions appear important for some of the macrocycle tetraamide complex conformations. NBO analysis indicates that the contribution to the overall stabilization of the complexes due to delocalization of the oxygen atoms' lone pairs into the cation increases as the metal ion gets farther away from both the phenyl and the ethene bridge units. The results of this work support the notion that macrocycle amides are promising alternatives for metal-ion binding. The Monte Carlo-based analysis with the PM3 semiempirical method suggests that the lithium ion complex prefer the C_{2v} conformation; however the Li-C_2 and Li-C_{2h} are also likely to occur. The PM3 conformational search did not find a conformer resembling the Li-C_s DFT geometry. Current efforts are directed toward the experimental realization of a macrocycle tetraamide based on the model structure considered here. Also of interest is the computational and experimental investigation of the binding selectivity of the proposed macrocycle tetraamide for the alkali and alkaline earth metal ions both in the gas phase and in solution.

Appendix A. Supplementary data

Cartesian coordinates for the B3LYP/6-31+G(d) optimized structures are available upon request via the internet at http:/pubs.acs.org. Also provided as supporting infor-

mation are Tables with the ab initio energies of all the structures in this work. Supplementary data associated with this article can be found, in the online version, at doi:10.1016/j.theochem.2007.05.024.

References

[1] (a) J.-M. Lehn, Supramolecular Chemistry, VCH, Weinheim, 1995;
(b) H.-J. Schneider, A. Yatsimirsky, Principles and Methods in Supramolecular Chemistry, Wiley, Chichester, 2000;
(c) J.W. Steed, H.L. Atwood, Supramolecular Chemistry, Wiley, Chichester, 2000;
(d) B. Dietrich, P. Viout, J.-M. Lehn, Macrocyclic Chemistry, VCH, Weinheim, 1993;
(e) A. Bianchi, K. Bowman-James, E. Garcia-España (Eds.), Supramolecular Chemistry of Anions, Wiley-VCH, New York, 1997;
(f) Y. Inoue, G.W. Gokel, Cation Binding by Macrocycles, Marcel Dekker, New York, 1990;
(g) E.C. Constable, Metals and Ligand Reactivity, VCH, Weinheim, 1995;
(h) M.T. Rodgers, P.B. Armentrout, J. Am. Chem. Soc. 122 (2000) 8548.
[2] (a) M. Brynda, T.A. Wesolowski, K. Wojciechowski, J. Phys. Chem. A 108 (2004) 5091;
(b) A. Casnati, A. Pochini, R. Ungaro, F. Ugozzoli, F. Arnaud, S. Fanni, M.J. Schwing, R.J.M. Egberink, F. de Jong, D.N. Reinhoudt, J. Am. Chem. Soc. 117 (1995) 2767.
[3] A. Minta, R.Y. Tsien, J. Biol. Chem. 264 (1989) 19449.
[4] (a) M. Castro, J. Cruz, E. Otazo-Sánchez, L. Perez-Marín, J. Phys. Chem. A 107 (2003) 9000;
(b) E. Bakker, P. Bühlmann, E. Pretsch, Chem. Rev. 97 (1997) 3083;
(c) E. Malinowska, J. Jurczak, T. Stankiewicz, Electroanal. 5 (1993) 489.
[5] (a) C.J. Pedersen, J. Am. Chem. Soc. 89 (1967) 2495;
(b) C.J. Pedersen, Angew. Chem., Int. Ed. Engl. 27 (1988) 1021;
(c) E.D. Glendening, D. Feller, M.A. Thompson, J. Am. Chem. Soc. 116 (1994) 10657;
(d) E.D. Glendening, D. Feller, J. Am. Chem. Soc. 118 (1996) 6052;
(e) A.L. Sargent, B.J. Mosley, J. W Sibert, J. Phys. Chem. A 110 (2006) 3826;
(f) E. Malinowska, W. Wróblewski, R. Ostaszewski, J. Jurczak, Polish J. Chem. 74 (2000) 701;
(g) K. Yamada, Y. Nomura, D. Citterio, N. Iwasawa, K. Suzuki, J. Am. Chem. Soc. 127 (2005) 6956.
[6] (a) J.-M. Lehn, Acc. Chem. Res. 11 (1978) 49;
(b) K.M. Tawarah, M.A. Khasawneh, S.A. Mizyed, J. Incl. Phenom. Macro. Chem. 51 (2005) 143;
(c) T. Kirichenko, V. Vetrogon, S. Scherbakov, N. Lukyanenko, Anal. Chim. Acta 505 (2004) 277.
[7] C. Cui, S.J. Cho, S. Kim, J. Phys. Chem. A 102 (1998) 1119.
[8] W.Y. Lee, C.H. Park, S. Kim, J. Am. Chem. Soc. 115 (1993) 1184.
[9] J. Szejtli, T. Osa, Comprehensive Supramolecular Chemistry, in: J.L. Atwood, J.E.D. Davies, D.D. MacNicol, F. Vögtle (Eds.), Cyclodextrines, Vol. 3, Elsevier, Oxford, 1996.
[10] (a) A. Casnati, L. Baldini, N. Pelizzi, K. Rissanen, F. Ugozzoli, R. Ungaro, J. Chem. Soc. Dalton Trans. 341 (2000);
(b) M. Perrin, D. Oehler, Calixarenes a Versatile Class of Macrocyclic Compounds, in: J. Vicens, V. Böhmer (Eds.), Kluwer Academic Publishers., Dordrecht, 1991;
(c) K. No, J.H. Lee, S.H. Yang, K.H. Noh, S.W. Lee, J.S. Kim, Tetrahedron 2403 (2003).
[11] (a) M. Chmielewski, J. Jurczak, Tetrahedron Lett. 45 (2004) 6007;
(b) M. Chmielewski, A. Szumna, J. Jurczak, Tetrahedron Lett. 45 (2004) 8699;
(c) Md.A. Hossain, S.O. Kang, D. Powell, K. Bowman-James, Inorg. Chem. 42 (2003) 1397;
(d) A. Szumna, D.T. Gryko, J. Jurczak, Heterocycles 52 (2002) 361;
(e) A. Szumna, J. Jurczak, Eur. J. Org. Chem. 4031 (2001);
(f) Md.A. Hossain, J.M. Llinares, D. Powell, K. Bowman-James, Inorg. Chem. 40 (2001) 2936;
(g) A. Szczepańska, P. Tarnowski, J. Jurczak, Polish J. Chem. 79 (2005) 1909;
(h) A. Szczepańska, P. Sałański, J. Jurczak, Tetrahedron 4775 (2003);
(i) H.-J. Choi, M.-K. Kwak, J.-M. Kim, Tetrahedron Lett. 38 (1997) 6217;
(j) M. Shakir, S.P. Varkey, P.S. Hameed, Polyhedron 12 (1993) 2775;
(k) H. Hioki, C. Still, J. Org. Chem. 63 (1998) 904;
(l) A. Chaudary, A. Phor, S. Sharma, A. Gajraj, R.V. Singh, Metal-Based Drugs 9 (2002) 97.
[12] (a) S.B. Suh, C. Cui, H.S. Son, J.S. U, Y. Won, K.S. Kim, J. Phys. Chem. B 106 (2002) 2061;
(b) H. Huang, L. Mu, J. He, J.-P. Cheng, Tetrahedron Lett. 43 (2002) 2255;
(c) K.S. Kim, C. Cui, S. Cho, J. Phys. Chem. B 102 (1998) 461.
[13] H.Y. Kim, J. Calabrese, C. McEwen, J. Am. Chem. Soc. 118 (1996) 1545.
[14] D.A. Dixon, K.D. Dobbs, J.J. Valentinii, J. Phys. Chem. 98 (1994) 13435.
[15] R.D. Parra, B. Yoo, M. Wemhoff, J. Phys. Chem. A 110 (2006) 4487.
[16] M.J. Frisch, G.W. Trucks, H.B. Schlegel, G.E. Scuseria, M.A. Robb, J.R. Cheeseman, J.A. Jr. Montgomery, T. Vreven, K.N. Kudin, J.C. Burant, J.M. Millam, S.S. Iyengar, J. Tomasi, V. Barone, B. Mennucci, M. Cossi, G. Scalmani, N. Rega, G.A. Petersson, H. Nakatsuji, M. Hada, M. Ehara, K. Toyota, R. Fukuda, J. Hasegawa, M. Ishida, T. Nakajima, Y. Honda, O. Kitao, H. Nakai, M. Klene, X. Li, J.E. Knox, H.P. Hratchian, J.B. Cross, V. Bakken, C. Adamo, J. Jaramillo, R. Gomperts, R.E. Stratmann, O. Yazyev, A.J. Austin, R. Cammi, C. Pomelli, J.W. Ochterski, P.Y. Ayala, K. Morokuma, G.A. Voth, P. Salvador, J.J. Dannenberg, V.G. Zakrzewski, S. Dapprich, A.D. Daniels, M.C. Strain, O. Farkas, D.K. Malick, A.D. Rabuck, K. Raghavachari, J.B. Foresman, J.V. Ortiz, Q. Cui, A.G. Baboul, S. Clifford, J. Cioslowski, B.B. Stefanov, G. Liu, A. Liashenko, P. Piskorz, I. Komaromi, R.L. Martin, D.J. Fox, T. Keith, M.A. Al-Laham, C.Y. Peng, A. Nanayakkara, M. Challacombe, P.M.W. Gill, B. Johnson, W. Chen, M.W. Wong, C. Gonzalez, J.A. Pople, Gaussian 03, Revision C.02. Gaussian, Inc.: Wallingford, CT, 2004.
[17] (a) P.J. Stephens, F.J. Devlin, C.F. Chabalowski, M.J. Frisch, J. Phys. Chem. 98 (1994) 11623;
(b) A.D. Becke, J. Chem. Phys. 98 (1993) 5648.
[18] P.C. Hariharan, J.A. Pople, Theor. Chim. Acta 28 (1973) 213.
[19] T. Clark, J. Chandrasekhar, G.W. Spitznagel, P.v.R. Schleyer, J. Comput. Chem. 4 (1983) 294.
[20] (a) J.-P. Blaudeau, M.P. McGrath, L.A. Curtiss, L. Radom, J. Chem. Phys. 107 (1997) 5016;
(b) A.D. McLean, G.S. Chandles, J. Chem. Phys. 72 (1980) 5639;
(c) R. Krishnan, J.S. Binkley, R. Seeger, J.A. Pople, J. Chem. Phys. 72 (1980) 650.
[21] C. Møller, M.S. Plesset, Phys. Rev. 46 (1934) 618.
[22] (a) J.P. Foster, L.A. Curtiss, F. Weinhold, J. Am. Chem. Soc. 102 (1980) 7211;
(b) A.E. Reed, L.A. Curtiss, F. Weinhold, Chem. Rev. 88 (1988) 899;
(c) E.D.Glendening, A.E. Reed, J.E.Carpenter, F. Weinhold, NBO version 3.1.
[23] S.F. Boys, F. Bernardi, Mol. Phys. 19 (1970) 553.
[24] Spartan'04 and Spartan'06, Wavefunction Inc., Irvine, CA.